Photovoltaic effect in the $La_{0.67}Ca_{0.33}MnO_3/LaMnO_3/SrTiO_3$:Nb heterojunctions with variant $LaMnO_3$ layers

A. D. Wei, J. R. Sun,[a] W. M. Lü, and B. G. Shen
Beijing National Laboratory for Condensed Matter Physics and Institute of Physics, Chinese Academy of Sciences, Beijing 100080, People's Republic of China

(Received 19 June 2009; accepted 13 July 2009; published online 3 August 2009)

Influence of $LaMnO_3$ layer, 0–12 nm in thickness, on photovoltaic effect (PVE) has been experimentally studied for the $La_{0.67}Ca_{0.33}MnO_3/LaMnO_3/SrTiO_3$:Nb junction. Presence of $LaMnO_3$ causes an obvious weakening of the PVE, demonstrated by the reduction in the carrier density excited by each photon. The interfacial barrier deduced from the PVE shows a rapid growth, from ~1.22 to ~1.45 eV, as the layer thickness increases from 0 to 2 nm, and saturates at ~1.5 eV above 2 nm. On the contrary, current-voltage characteristics suggest a smooth reduction in interfacial barrier with layer thickness. These results can be quantitatively understood assuming the occurrence of a notch and a spike in the conduction band edges at the interface of the junction.
© *2009 American Institute of Physics*. [DOI: 10.1063/1.3194776]

Heterojunctions are different from homojunctions in many aspects.[1] The different band structures of the two components forming the diodes allow a band structure tailoring on the demand of fundamental research or practical application. This provides an important degree of freedom that produces many interesting phenomena. Manganites and $SrTiO_3$:Nb are different in energy bands. As reported, the band gap/electron affinity is ~3.2 eV/3.9 eV for $SrTiO_3$ and ~0.5 eV/4.9 eV for hole-doped manganites.[2] Therefore, the junctions composed of manganites and $SrTiO_3$:Nb are typical heterojunctions. The manganite junctions are found to exhibit many distinctive characters such as good rectifying property,[3] bias-dependent magnetoresistance,[4] and unusual photovoltaic effect.[5] However, all these phenomena can be explained simply based on the theory for homojunctions. It is fortunate that, by introducing a proper inventing layer, we obtained the junctions that show the typical features of heterojunctions.[6] Unlike homojunctions, $La_{0.67}Ca_{0.33}MnO_3/LaMnO_3/SrTiO_3$:0.05 wt %Nb (LCMO/LMO/STON) experiences two different processes that can be well described by the theory developed by assuming the occurrence of a notch and a spike in the conduction band edges at the interface of the diode, due to the band mismatch between LMO, LCMO, and STON. In fact, in addition to the two-step current (I)-voltage (V) characteristics, other unusual effects are also possible in the junction with a complex band structure. Among them, the photovoltaic effect (PVE), which caries the very information on band structure, is especially attractive. As well established, extra carriers can be produced by photon excitation, forming photocurrent (I_L) if they have enough energy to conquer interfacial barrier. It is obvious that the special band structure in LCMO/LMO/STON, if exists, should have a direct reflection in the PVE. Based on this consideration, in this latter, we performed a systematic study on the influence of the LMO layer on the PVE of LCMO/LMO/STON.

The samples were fabricated by growing first a LMO layer with a thickness between $t=0$ and 12 nm then a LCMO layer of ~150 nm on a 0.05 wt %Nb-doped $SrTiO_3$ substrate (STON) using pulsed laser ablation technique.[6] The buffer layer is quite smooth with a terracelike surface structure, as revealed by the atomic force microscope analysis. The root-mean-square roughness of the LMO layer of, for example, 8 nm is ~0.3 nm, with a peak-to-valley fluctuation of ~0.5 nm. X-ray diffraction analysis shows a small increase in the out-of-plane lattice constant of LCMO, from ~0.5387 nm for $t=0$ to ~0.5398 nm for $t=8$ nm.

Two Cu pads were deposited, also by laser ablating, respectively on LCMO and STON as electrodes (junction area=1×1 mm^2). The resistance is ~10 Ω for the Cu-STON contact and ~100 Ω for the Cu-LCMO contact. The I-V characteristics were measured by a superconducting quantum interference device magnetometer equipped with a resistance measurement unit. The direction directs from LCMO to STON is positive.

The transport behaviors of the junctions with different LMO buffer layers and corresponding analyses can be found in Ref. 6. The I-V characteristics exhibit a gradual evolution with the thickness of the LMO layer. Unlike the junctions for $t<6$ nm, the junction for $t=6$ or 8 nm shows a two-step electronic process, which signifies the appearance of a complex band structure. In Fig. 1(a) we show the results for $t=8$ nm for reference.

It is obvious that the interfacial potential Φ_B is the key factor affecting the physical properties of the junctions. The Shockley character of the I-V characteristics allows the determination of Φ_B with the use of the relation $J_S \propto T^2 \exp(\Phi_B/k_BT)$, where J_S is the saturation current and k_B the Boltzmann constant. To first approximation, LCMO/STON can be treated as a Schottky junction. In the presence of a LMO layer, $(1-1/n)V$ is dropped across the insulating layer and V/n is applied to the depletion layer (n is the ideality factor). This means, according to Yamamoto *et al.*,[7] that the I-V curves of LCMO/LMO/STON are similar to those of LCMO/STON after describing the effect of the insulating layer by ideality factor. Figure 1(b) presents the interfacial barrier for the junctions with $t=0$, 1, 2, 4, 6, and 8 nm. The interfacial barrier in the junction with a LMO layer thicker than 8 nm cannot be obtained in this way due to the

[a]Author to whom correspondence should be addressed. Electronic mail: jrsun@g203.iphy.ac.cn.

0003-6951/2009/95(5)/052502/3/$25.00 © 2009 American Institute of Physics

Downloaded 14 Aug 2009 to 159.226.36.175. Redistribution subject to AIP license or copyright; see http://apl.aip.org/apl/copyright.jsp

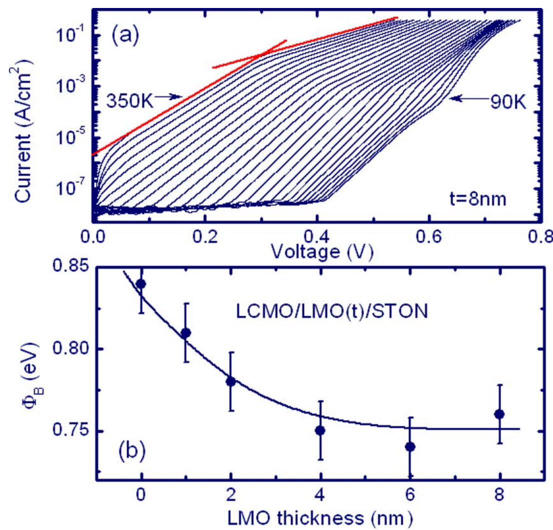

FIG. 1. (Color online) (a) Semilogarithmic plot of the current-voltage characteristics of LCMO/LMO(8 nm)/STON and (b) the interfacial barrier derived from the *I-V* curves. Errors of Φ_B are due to the uncertainty of the saturation current. Solid lines are guides for the eyes.

appearance of severe leakage current. The interfacial barrier is ~0.84 eV for $t=0$ and ~0.76 eV for $t=8$ nm, decreasing smoothly with the increase in the LMO layer thickness. The interfacial barrier is derived for the low bias process when two electronic processes occur. As we know, LMO/STON exhibits a lower Φ_B than that of LCMO/STON due to the high Fermi level of LMO. With this in mind, the reduction in interfacial barrier in LCMO/LMO/STON is plausible. However, the results here may not be a complete description for the complex electronic structure of the junctions, especially in the presence of two interfacial barriers.

As well established, electrons in LCMO can be excited by photons and penetrate through the junction region under the driving of the built-in electric field if $h\upsilon \geq \Phi_B$, yielding photocurrent, where h is the Planck constant, and υ the light frequency. According to Fowler,[8] there is a simple relation between the quantum efficiency and photon energy, $R \propto (h\nu - \Phi_B)^2$, when $|h\upsilon - \Phi_B| \geq 3k_BT$. Based on this relation Φ_B can also be derived from the PVE.

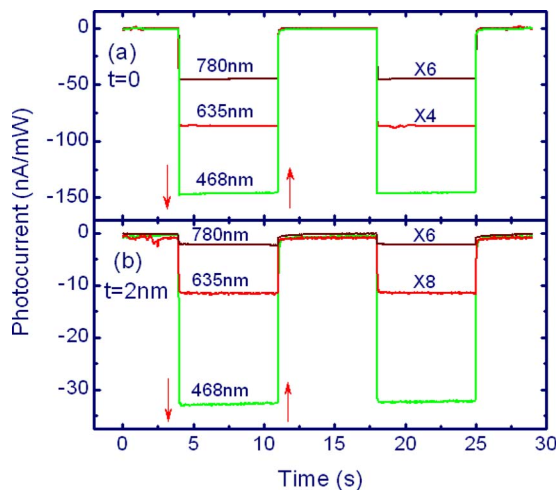

FIG. 2. (Color online) Selected photocurrent of the LCMO/LMO(t)/STON junctions with $t=0$ (a) and 2 nm (b), measured under the light power of 1 mW and different wavelengths. Arrows signify the positions of light on and off.

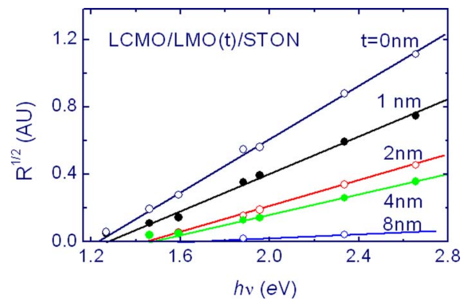

FIG. 3. (Color online) Square root quantum efficiency as a function of photon energy for the LCMO/LMO(t)/STON junctions. Solid lines are guides for the eyes.

Lasers with the wavelengths between 450 and 1000 nm were used in the present experiment. The spot size of the incident light is ~1 mm in diameter. As a representative, Figs. 2(a) and 2(b) show the photocurrents produced by the lights of 468, 635, and 780 nm for the junctions of $t=0$ and 2 nm. Sudden jumps in photocurrent are observed for the laser on and off, signifying a swift response of I_L to light illumination. Two distinctive features can be identified from the data in Fig. 2. First, for an identical junction, the light with a shorter wavelength yields a stronger photoresponse. For example, the photocurrent in LCMO/STON is ~146 and ~45 nA/mW for the wavelengths of 468 and 780 nm, respectively. Second, photocurrent weakens as layer thickness increases if light parameters are fixed. For example, the photocurrent, under the light of 468 nm, decreases from ~146 to ~33 nA/mW as t grows from 0 to 2 nm. The former manifests the presence of interfacial barrier, only the photons with the energy well above Φ_B are effective, and the latter suggests a change of this barrier with the LMO layer thickness.

Figure 3 presents square root R as a function of $h\nu$. Satisfactory linear $R^{1/2}-h\upsilon$ relations are observed for all samples, indicating the presence of definite interfacial barriers in the junctions. The most remarkable result is the high energy shift of the intercept of the $R^{1/2}-h\nu$ curve on the $h\nu$-axis, which indicates the growth of interfacial barrier, and the accompanying declining of the $R^{1/2}-h\nu$ slope as the LMO layer thickness increases. These changes are severe when t is small and slow down when $t>2$ nm. The interfacial barrier deduced from the Fowler equation, denoted as Φ_{BP}, is illustrated in Fig. 4. It exhibits a strong dependence on LMO layer, rising from ~1.22 to ~1.48 eV as t increases from 0 to 2 nm and saturating at ~1.5 eV above 2 nm. Compared with Φ_B, two remarkable features can be identified. The first one is the different dependence of Φ_{BP} on

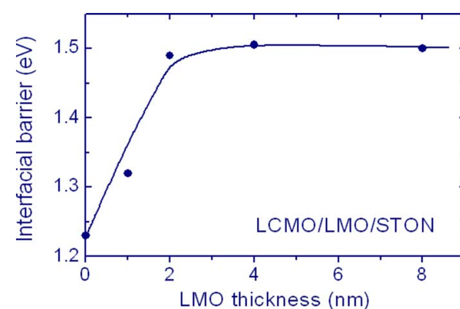

FIG. 4. (Color online) Interfacial barrier, derived from photovoltaic effect, as a function of the layer thickness of LMO. Solid line is a guide for the eyes.

Downloaded 14 Aug 2009 to 159.226.36.175. Redistribution subject to AIP license or copyright; see http://apl.aip.org/apl/copyright.jsp

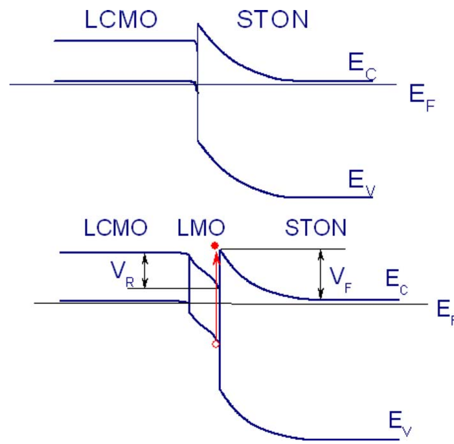

FIG. 5. (Color online) A schematic band structure of the manganite junction. Arrow in the figure indicates the excitation of extra charge carriers.

layer thickness and the second one is the significantly large Φ_{BP} value.

We have studied the effect of the film thickness of LCMO on the PVE for the LCMO/STON junctions,[9] and found a dramatic enhancement of the PVE as film thickness grows from 5 to 50 nm and a saturation above 50 nm, due to the relaxation of tensile stress of the film. The film thickness of the present junctions is above 150 nm. Although the introduction of the LMO layer causes an increase in the out-of-plane lattice constant of LCMO, the change is too small to yield any detectable effects on Φ_{BP}.

According to the semiconductor theory, the Schottky barriers derived from the *I-V* curves and the PVE, respectively, should be the same within 0.02 eV.[1] However, when leakage current or tunneling current appears, usually a low Φ_B is obtained. The junctions studied here could be of high quality noting the negligible deviation of their ideality factors from unity and the extremely high junction resistance. The near temperature independence of the ideality factor between 200 and 350 K further indicates the dominant role of the thermionic emission process in the junction. Therefore, the difference between Φ_{BP} and Φ_B cannot be simply ascribed to the effect of tunneling and/or leakage current.

As proved by the *I-V* analysis, an energy band structure characterized by notch-and-spike-shaped conduction band edges may exist in the junction (Fig. 5). In this case, two distinctive energy barriers can be derived respectively from the two *I-V* fragments in the low and high bias range. Complex band structure may also exist in the junctions without obvious two-step features and the data in Fig. 1 could be the energy barrier in STON. In contrast, in the PVE experiment, charge carriers come from LCMO or LMO, and the barrier height faced by them is measured from the downward bended valence band (it is possible noting the presence of a dead layer in LCMO), instead of Fermi level as in Schottky junctions (Fig. 5). As a result, the required energy is significantly larger than expected. As well established, in STON the Fermi level (E_F) is close to the bottom of the conduction band (E_C), while it is slightly below the top of the valence band (E_V) in LCMO. Therefore, the barrier height will be $\Phi_{BP}=E_C(\text{STON})-E_V(\text{LCMO})$ for LCMO/STON. If LCMO can be treated as idealized metal, $\Phi_{BP}=E_C(\text{STON})-E_F(\text{LCMO})=\Phi_B$ ($E_F \approx E_V$). However, if LCMO deviates severely from metal or, equivalently, its band bending is obvious, $\Phi_{BP}=E_C(\text{STON})-E_V(\text{LCMO})>\Phi_B$ since $E_F>E_V$ at the interface. This explains the difference between Φ_B and Φ_{BP}. As we know, the energy gap of LCMO is ~0.5 eV, and the band offset between LCMO and STON is $\Delta E_C \sim 0.6$ eV, adopting the work function of 4.9 eV for LCMO and 3.9 eV for $SrTiO_3$:Nb and ignoring the difference of E_F and E_V in LCMO. A direct calculation gives an interfacial barrier of ~1.1 eV. The agreement with the one derived from PVE (~1.2 eV) is good noting the ignorance of other factors affecting Φ_{BP} except for the work functions. Energy required by producing extra carriers in the region apart from the interface could be low due to the gradual band flattening. However, these carriers may have no significant contribution to PVE due to their annihilation on the way to interface.

Although the Fermi level of LMO is higher than that of LCMO,[10] $E_V(\text{LMO})$ is lower than $E_V(\text{LCMO})$,[11] which could cause a further downward bending of the conduction band, as shown in Fig. 5. When LMO is thick, nearly all of the carriers contributing to the PVE come from the valence band of LMO, the extra carriers from the corresponding band of LCMO have hardly opportunity to reach the LMO/STON interface. The steep increase of Φ_{BP} shows the rapid enhancement of the effect of the LMO layer from 0 to 2 nm. Above $t=2$ nm, Φ_{BP} stays at a constant value, which implies that 2 nm may be the free distance for nonequilibrium carriers. From Fig. 5, there is an approximate relation $\Phi_{BP} \approx V_R + V_F$. As reported, in the junctions $t=6$ nm and 8 nm the two interfacial barriers V_F and V_R can be, respectively, determined.[6] A direct calculation gives $V_F+V_R \approx 1.37$ eV for $t=6$ nm and $V_F+V_R \approx 1.34$ eV for $t=8$ nm, in reasonably consistent with the observed ~1.5 eV.

This work has been supported by the National Basic Research of China, the National Natural Science Foundation of China, the Knowledge Innovation Project of the Chinese Academy of Science, and the Beijing Municipal Nature Science Foundation.

[1]M. Sze, *Physics of Semiconductor Devices*, 2nd ed. (Wiley, New York, 1981).
[2]D. W. Reagor, S. Y. Lee, Y. Li, and Q. X. Jia, J. Appl. Phys. **95**, 7971 (2004); J. Robertson, J. Vac. Sci. Technol. B **18**, 1785 (2000).
[3]M. Sugiura, K. Uragou, M. Noda, M. Tachiki, and T. Kobayashi, Jpn. J. Appl. Phys., Part 1 **38**, 2675 (1999); H. Tanaka, J. Zhang, and T. Kawai, Phys. Rev. Lett. **88**, 027204 (2001).
[4]J. R. Sun, C. M. Xiong, T. Y. Zhao, S. Y. Zhang, Y. F. Chen, and B. G. Shen, Appl. Phys. Lett. **84**, 1528 (2004); N. Nakagawa, M. Asai, Y. Mukunoki, T. Susaki, and H. Y. Hwang, *ibid.* **86**, 082504 (2005).
[5]J. R. Sun, B. G. Shen, Z. G. Sheng, and Y. P. Sun, Appl. Phys. Lett. **85**, 3375 (2004); Z. G. Sheng, B. C. Zhao, W. H. Song, Y. P. Sun, J. R. Sun, and B. G. Shen, *ibid.* **87**, 242501 (2005).
[6]W. M. Lü, J. R. Sun, Y. Z. Chen, and B. G. Shen, Appl. Phys. Lett. **94**, 152514 (2009).
[7]T. Yamamoto, S. Suzuki, K. Kawaguchi, and K. Takahashi, Jpn. J. Appl. Phys., Part 1 **37**, 4737 (1998).
[8]R. H. Fowler, Phys. Rev. **38**, 45 (1931).
[9]W. M. Lü, A. D. Wei, J. R. Sun, Y. Z. Chen, and B. G. Shen, Appl. Phys. Lett. **94**, 082506 (2009).
[10]J.-H. Park, C. T. Chen, S.-W. Cheong, W. Bao, G. Meigs, V. Chakarian, and Y. U. Idzerda, Phys. Rev. Lett. **76**, 4215 (1996).
[11]T. Saitoh, A. E. Bocquet, T. Mizokawa, H. Namatame, A. Fujimori, M. Abbate, Y. Takeda, and M. Takano, Phys. Rev. B **51**, 13942 (1995).

Downloaded 14 Aug 2009 to 159.226.36.175. Redistribution subject to AIP license or copyright; see http://apl.aip.org/apl/copyright.jsp